Surface Forces in the Tapping Mode: Solvent Permeability and Hydrodynamic Thickness of Adsorbed Polymer Brushes

Ali Dhinojwala and Steve Granick*

Department of Materials Science and Engineering, University of Illinois, Urbana, Illinois 61801

Received January 9, 1996; Revised Manuscript Received July 16, 1996[⊗]

ABSTRACT: A surface forces apparatus modified to apply small-amplitude oscillatory displacements in the normal direction was used to measure the drainage of tetradecane (a good solvent) past polybutadiene (PB) brushes end-attached to two opposed mica surfaces. The PB was attached by selective adsorption of the poly(vinylpyridine) (PVP) block of a PB−PVP diblock copolymer. In-phase motion in the normal direction reflected elastic forces; these were found to be equivalent to the static force−distance profile measured directly. Out-of-phase motions reflected viscous flow of solvent since the PB chains did not contribute to dissipation over the oscillation frequencies studied. No frequency dependence was observed from 1 to 100 Hz. The hydrodynamic forces at a given plate separation (D) implied an effective plate separation less than D by a constant hydrodynamic thickness (R_H) but otherwise the flow of a Newtonian liquid with viscosity same as in the bulk. The value of the hydrodynamic thickness was less than the value (L_0) measured in the equilibrium force−distance profile, implying significant penetration of the velocity field into the brush layer. The value of R_H diminished monotonically as the plate separation was reduced from $4L_0$ to $0.2L_0$. In other language, the "slip plane" changed monotonically with decreasing film thickness. The magnitude of hydrodynamic forces grew in proportion to $D^{-1.2}$. This would be expected from scaling arguments for a Θ solvent but deviates decidedly from the prediced $D^{-0.5}$ from scaling arguments for semidilute good solvent conditions. This could reflect inapplicability of the Brinkman equation or could reflect different scaling behavior of the static and hydrodynamic screening lengths.

Introduction

Many of the most important uses of polymers at surfaces are in situations where surfaces are in relative motion toward or away from one another. This finds wide application to stabilize colloidal particles for a variety of technological applications.[1,2] In past work, the static repulsive forces for adsorbed or grafted polymer-coated surfaces have seen extensive theoretical and experimental investigation; the dependence of these static forces on molecular weight, surface coverage, and interaction energies is well documented.[3−14] Much less is known about polymer-coated surfaces in relative motion.

We are interested here in the influence of hydrodynamic forces due to drainage of solvent between polymer-coated surfaces in a good solvent. For typical Brownian motion of colloidal particles, the hydrodynamic forces could often exceed the static forces and could prevent the complete drainage of solvent even before the particle separation became small enough for the polymer layers to overlap. Thus hydrodynamic forces could have interesting consequences for the stability and rheology of colloidal particles.

Traditionally, the presence of adsorbed or grafted polymers is accounted for by simply taking the classical Reynolds equation for describing hydrodynamic forces[15] and subtracting, from the actual solid−solid distance, the effective thickness of the immobilized polymer layer. This is often referred to as hydrodynamic thickness.[16−18] This patchwork approach works if the solid−solid separation is much greater than the hydrodynamic thickness. However, at lesser separations, even if polymer−coated surfaces do not touch one another, hydrodynamic forces are found experimentally to be smaller than expected from such a modified Reynolds equation.[16−18]

Thus an adsorbed polymer layer or a brush is far from a rigid substrate. In fact, at small separations the hydrodynamic forces can be large enough to influence the penetration of the solvent velocity field within the adsorbed layer, as we shall see from the study below. In other language, the "slip plane"[16] changes with film thickness. Local deformations of the underlying substrate, owing to compression by the hydrodynamic forces, also come into play.[19]

Interesting theories have modeled the flow of solvent between grafted polymer layers using the analogy of flow through a porous medium.[20−22] If surfaces are far apart, the presence of polymer is accounted for by assuming a constant hydrodynamic thickness. If the surface separation is less than the total unperturbed brush thickness, the pore size for solvent flow is considered to be the static correlation length. Fredrickson et al.[21] used scaling laws for semidilute good solvent conditions and an assumed step profile of brush concentration, to predict that the hydrodynamic force should scale as $D^{-0.5}$, where D is the closest separation between a sphere and a flat plane. Although an experiment designed to test this theory concluded that theory was verified by experiment,[17] the point is difficult to understand intuitively since $D^{-0.5}$ scaling is so much weaker than D^{-1} scaling in pure solvent. This implication, counterintuitive to us, prompted the present study.

Experimental Section

The diblock copolymers of polybutadiene and poly(vinylpyridine) (PB−PVP) were generously donated by Professor H. Watanabe of the Institute of Chemical Research at Kyoto University. The molecular weights were 38 500 (PB) and 23 700 (PVP). The ratio weight-average to number-average molecular weight was $M_w/M_n < 1.05$.

Solutions were prepared in toluene far below the critical micelle concentration, at concentrations 5−10 μg/mL. To ensure complete dissolution, the solutions had to be made at least 24 h before the subsequent adsorption process. Freshly cleaved sheets of muscovite mica were first calibrated in a

[⊗] Abstract published in *Advance ACS Abstracts,* January 1, 1997.

S0024-9297(96)00027-7 CCC: $14.00

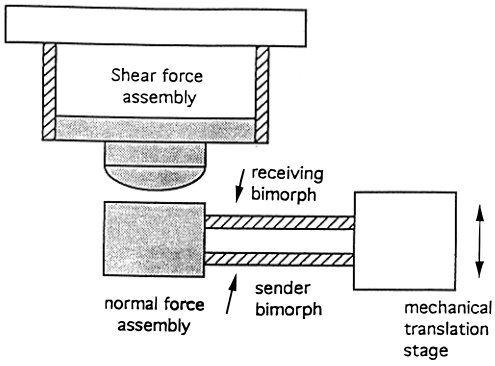

Figure 1. Schematic diagram of the apparatus to measure shear and normal forces concurrently. The top surface was attached to a shear force assembly, described elsewhere.[23] In this new device, the bottom surface was similarly attached to two piezoelectric bimorphs that were oriented at right angles to the normal line between the two surfaces. An oscillatory normal force was generated by applying voltage to the bottom piezoelectric bimorph (the "sender"). This was resisted by the sample, and the actual time-dependent deflection of the bottom surface was monitored from the time-dependent voltage that was induced in the top bimorph (the "receiver").

surface forces apparatus to determine the mica thickness and then immersed in the polymer solution for 2 h. Since toluene is a nonsolvent for the PVP block but a good solvent for the PB block, the block polymers adsorbed onto the mica by selective adsorption of the PVP block. After adsorption, to rinse off nonadsorbed chains, the coated mica sheets were soaked in pure toluene for at least 2 h. Finally, the dried polymer-coated sheets were mounted into the experimental apparatus and a droplet of tetradecane was placed between the mica sheets by pipett. The experimental temperature was 24 °C.

Within the surface forces apparatus described previously,[23] small-amplitude oscillatory normal forces were applied using the double-cantilever bimorph assembly shown schematically in Figure 1. The bottom cylindrical lens was supported on the normal force assembly. A small-amplitude (corresponding to a displacement of 0.5−1 nm) oscillatory force was applied to the bottom piezoelectric bimorph while the resulting displacement was monitored by the top bimorph. Analysis of the data was analogous to that for shear experiments.[23] In particular, the damping and phase shift of the oscillation can be related to the elastic and viscous force constant as follows:[23,24]

$$\omega b = K_{sp}A_0 \sin(\theta)/A \quad (1)$$

$$k = K_{sp}(A_0 \cos(\theta)/A - 1) \quad (2)$$

where A is the displacement in the presence of liquid, A_0 is the maximum displacement when the surfaces are separated in air, θ is the phase difference between the output when the surfaces are separated in air to that in the presence of liquid, and K_{sp} is the effective spring constant of the normal force assembly. Equations 1 and 2 hold for measurements below the resonance frequency of the normal force assembly.

In the experiments presented here, $K_{sp} = 1 \times 10^4$ N/m. The magnitude of K_{sp} was determined from the resonance frequency of the spring assembly and its known mass. The resonance frequency was 235 Hz.

Linear response, obtained with oscillation amplitudes of 10 Å or less, was verified.

Results and Discussion

The squeeze flow of solvent between brush-tethered mica surfaces is an elelastohydrodynamic problem. We begin by describing characterization of the brush layers and analysis of the dynamic oscillatory data. We then discuss the hydrodynamic and static forces, respectively. Finally, we discuss effects of frequency.

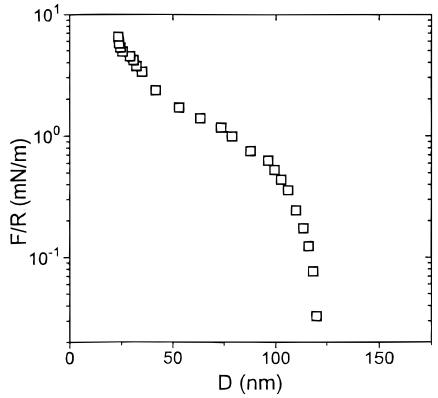

Figure 2. Static force, F, normalized by the mean radius of curvature, R, of the crossed cylindrical surfaces plotted logarithmically against surface separation.

Characterization of the Brush Assembly. To make contact with numerous past discussion of static force−distance profiles,[3−14] this was measured first. In Figure 2, force normalized by the mean radius of curvature of the crossed mica cylinders is plotted against mica−mica separation on semilogarithmic scales. The data is monotonically repulsive and its force−distance relations can be fit quantitatively to expectations.[3−14] The onset of measurable surface forces occurred at $2L_0 = 1250$ Å, implying a thickness $L_0 = 625$ Å per unperturbed brush layer.

To determine the surface coverage, the thickness of the dry PB−PVP layers was measured by multiple-beam interferometry after completing the experiments. It is true that from comparison with the simplest theory for these systems, the Alexander−de Gennes theory, one deduces from the experimental measurement of L_0 that the average spacing between anchor groups was $\delta = 46$ Å. Direct measurement was believed to be more reliable than comparisons to theory for the observed force−distance profile. The polymer-coated surfaces were removed from the surface forces apparatus, rinsed with toluene, and dried under dry argon gas for at least 3 h. The dry layer thickness was 31 ± 4 Å, which corresponds to a surface excess of 1.5 mg/m^2 calculated from the known density. This in turn corresponded to $\theta = 2.3 \times 10^{16}$ chains/m^2, an average spacing between anchor points of $\delta = 65$ Å.

Analysis of Data. For a Newtonian fluid, elastic forces in the frequency range studied should be negligible. However, for adsorbed polymer layers or a brush, the elastic force contribution is significant when the opposed layers touch each other, as shown by Figure 2. There will be an additional contribution to the elastic forces due to the compliance of the device or of the glue used to mount the mica surfaces onto the device.

To separate these contributions, a spring−dashpot model was used for convenience. The contribution from the device or glue was considered to be purely elastic, a spring constant k_g; this was confirmed independently with bare mica surfaces in adhesive contact. From this calibration, the k_g was determined to be $(1.0 \pm 0.2) \times 10^5$ N/m, independent (over our frequency range) of frequency.

The respective contributions of the hydrodynamic forces of the sample (an out-of-phase response), the static forces of the sample (an in-phase response), and the device itself (k_g) were then separated by the model sketched in Figure 3. Here the sample comprised a parallel combination of in-phase response (a spring

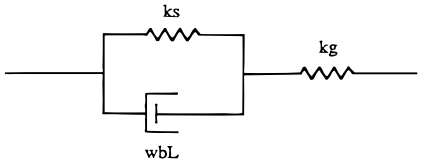

Figure 3. Equivalent mechanical circuit to model the parallel contributions of viscous force (ωb_L) and static force (k_s) due to sample in serial combination with the elastic compliance of the device or glue (k_g).

constant) and out-of-phase response (a dashpot). The choice of these two elements in parallel was dictated by the need that the sample undergo the same displacement for the elastic and dissipative forces.

Hydrodynamic (Out-of-Phase) Forces. The hydrodynamic force for a sphere approaching a flat surface at a constant velocity, v, can be expressed using the Reynolds equation as follows:[15]

$$F_H = 6\pi R^2 \eta v/D \tag{3}$$

where R is the radius of the sphere, η is the viscosity, and D is the closest separation between the sphere and the flat surface. For an oscillatory normal force, the hydrodynamic force constant can be written as

$$\omega b_L = 6\pi R^2 \omega \eta/D \tag{4}$$

where b_L is an equivalent dashpot coefficient. For quantitative comparison to data, it is common to rewrite eq 4 as follows:

$$G = 6\pi R^2 \omega/(\omega b_L) = D/\eta \tag{5}$$

Thus if G is plotted as a function of distance for a Newtonian fluid, the slope is the inverse viscosity and the intercept is twice the hydrodynamic thickness. The latter, for small molecules, is typically 5−10 molecular diameters.[18,25,26]

It is essential to note that eq 5 involves only the hydrodynamic force contribution, ωb_L—not the total force as assumed in a previous[17] study. If this distinction is not made, the magnitudes of hydrodynamic forces are overestimated. This is a particular problem at small surface−surface separations, where in-phase (elastic) forces make the largest contributions to the total.

In Figure 4, having made this separation of dissipative forces from the total, we plot G as a function of surface−surface separation for two cases: bare mica surfaces immersed in pure tetradecane, and PVP−PB brushes in tetradecane. As should be expected, the slope of the plot is the same provided that D is large enough, indicating that the viscosity of the liquid was that of pure tetradecane. Specifically, $\eta = 2.3$ cP. For the drainage of pure tetradecane, the intercept at 2 nm corresponded to a thickness of approximately 5 molecular diameters, as expected. But in the case of drainage of tetradecane between brushes, significant deviations from linearity appeared at $D < 400$ Å.

The actual magnitude of hydrodynamic forces is perhaps easier to understand intuitively. Therefore for comparison, the bottom panel of Figure 4 shows this quantity, $1/G$, plotted against surface−surface separation. One sees that hydrodynamic forces were indeed larger for brush-covered surfaces. The modification of fluid flow by polymer is less obvious in this form of representation, however.

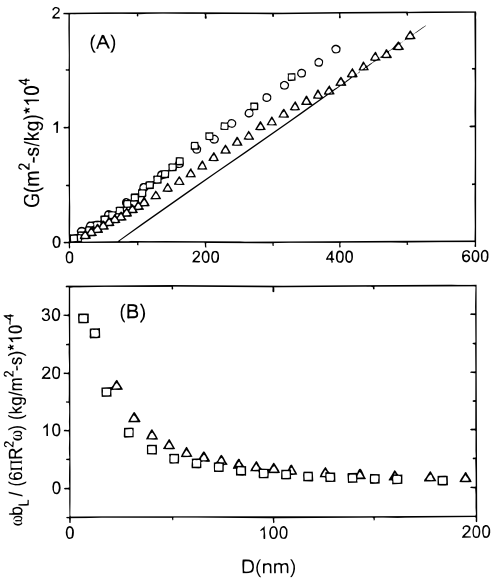

Figure 4. (A) Viscous damping function, G (of order 10^{-4} m^2-s/kg), plotted against surface separation for pure tetradecane squeezed between mica surfaces (squares, 0.25 Hz; circles, 7.5 Hz) and for pure tetradecane squeezed between surfaces coated with PVP−PB brushes (triangles, 10 Hz). The straight line corresponds to the known viscosity of tetradecane, 2.2−2.3 cP. These values of G correspond to forces of order 10^{-7} N. (B) Same data as in (A) plotted as hydrodynamic force constant, $1/G$, as a function of surface separation.

Analysis of Solvent Flow at Large Separations. For the pure solvent, the Reynolds equation fit well even without correcting D for the intercept at small solvent thickness. For the brush layers, the hydrodynamic forces fit the Reynolds equation with separation ($D - 2R_H$), where R_H was an equivalent hydrodynamic thickness chosen to fit the data. The value of R_H was 40 ± 10 nm, i.e. only two-thirds of the unperturbed brush thickness, at even the largest separations studied.

It is interesting that this implied so much penetration of the solvent flow within the brush itself. The finding agrees qualitatively with the predictions by Milner,[20] which combined the Brinkman equation with an assumed parabolic brush density profile. However, this large penetration contrasts with the prediction of ref 21—thus demonstrating the need to use a more detailed brush density profile then the step profile used in those calculations.

Analysis of Solvent Flow at Small Separations. What happened when the brushes were compressed to less than their unperturbed thickness? Fredrickson et al.[21] proposed an analogy between solvent flow through the compressed brush layer and creeping flow through a porous medium.[27] The hydrodynamic force was then written as

$$\omega b_L \propto (\eta \omega R^2)/D(D/\xi(D))^2 \tag{6}$$

where ξ is the hydrodynamic screening length. Using the scaling arguments for good solvents in a semidilute solution, $\xi \propto D^{0.75}$, and a constant value of ξ throughout the crossed cylinder geometry, G was predicted to scale as $D^{0.5}$.[21]

The data from the top panel of Figure 4 are shown on magnified scales in Figure 5. Comparison to experiment is difficult because this predicted scaling was not observed. One approach was to seek the best least-squares fit to the data, shown as a dotted line in Figure 5. But this implies the counterintuitive result that flow

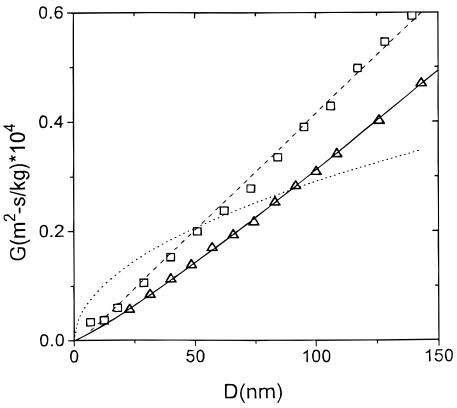

Figure 5. Blowup of the region 0−150 nm in Figure 4. The solid line is the best empirical fit, $G \propto D^{1.2}$. The dotted line is the best fit to the predicted $G \propto D^{0.5}$ (ref 21). The dashed line is the fit to the classical Reynolds equation for a Newtonian liquid, $G \propto D^{1.0\pm0.05}$.

of solvent at small D presented less hydrodynamic force through a polymer mesh than in its absence—the reverse of the observed behavior. A second approach was to arbitrarily draw the prediction to fall at lesser values of G, lower than for the pure solvent. But this would imply even larger numerical disagreement with the data.

Instead, the data suggest $G \propto D^{1.2}$ empirically. It is interesting that this apparent scaling is similar to what could be predicted for a semidilute solvent at Θ solvent conditions or more concentrated solutions ($\eta \alpha D$ and $G \propto D^1$). However, the average concentration in Figure 5 ranges from 2% (when the brush layers begin to touch each other) to 25% (largest compression). It was suggested that scaling $\eta \propto c^{-0.75}$ is difficult to observe and that the $\eta \propto c^{-1}$ scaling occupies a surprisingly large span of concentration range, even for very good solvents.[28] If eq 6 is valid, the intriguing differences of scaling behavior observed for static and hydrodynamic screening length for the same concentration range needs further explanation.

It is interesting to also note, in Figure 5, that the values of G approached zero smoothly as D approached zero. The earlier study by Klein et al.,[17] using polystyrene (PS) grafted brush layers, reported the values of G to vanish at separations close to 40 nm, equivalent to a polymer concentration of merely 15−20%. This was interpreted as confinement-induced solid-like behavior.[17] However, bulk PS at room temperature vitrifies at a much larger polymer concentration, around 85%.[28] In this study, we observed no intimation of solid-like behavior until the brushes were compressed to nearly the dry-layer thickness. This was also supported by the negligible shear resistance observed over these separations. We suspect that the apparent vanishing of G at unexpectedly large separations may be explained from failure to separate in-phase from out-of-phase forces in ref 17, thereby leading to overestimation of the hydrodynamic forces. It is then not necessary to postulate slowing down of the dynamics under confinement.

It is clear that the simplified picture of a constant hydrodynamic thickness did not hold at these separations. Here the hydrodynamic forces were strong enough to influence the penetration of the velocity field of the solvent or the structure of the brush layers. The total hydrodynamic force was probably a combination of increase in effective viscosity as well as reduction in effective hydrodynamic thickness.

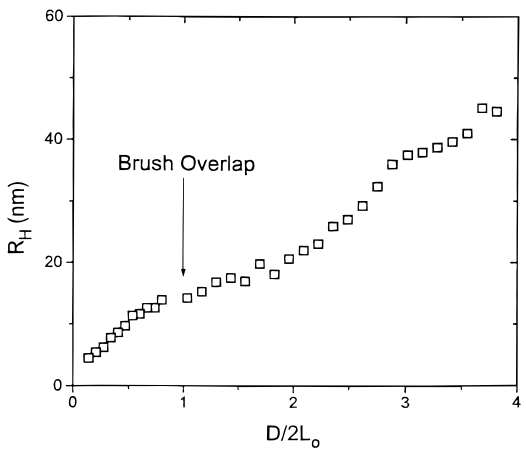

Figure 6. Equivalent hydrodynamic thickness, R_H, plotted against surface separation, D, normalized by the unperturbed brush thickness, L_0. The hydrodynamic thickness was calculated using the viscosity of tetradecane of 2.2−2.3 cP and eq 4 with $D_s = D - 2R_H$, where D is the surface separation.

Further Estimates of Hydrodynamic Thickness. It was interesting to also estimate an effective hydrodynamic thickness in the case that the brush separation was close to L_0 yet not touching. As a first approximation, we assumed that the solvent viscosity was unaffected by the presence of polymer (for discussion of this point, see the paragraph that follows). The results are shown in Figure 6. The x-axis is the ratio of the separation to the unperturbed thickness of the two brushes. At the largest separations, the R_H took the value, 40 nm, discussed in the previous section. At lesser separations, but starting even before the brushes touched one another, the R_H fell monotonically to lesser values, ultimately 20 nm and less. This amounted to a reduction by 70% from the unperturbed brush thickness, L_0. It is interesting to reflect on this and to note that the polymer brush layers were far from the rigid substrate assumed in simply applying the Reynolds equation to model the flow of solvent for these systems. A similar result would be expected in the case of adsorbed homopolymers.[29]

Estimates of Viscosity Changes. It may at first seem surprising that no dramatic changes of viscosity were implied, since it is obvious, in Figures 4 and 5, that the changes in slope as a function of thickness were rather small, at most only 2−3 times higher than the viscosity of pure tetradecane. On the other hand, the concentration of polymer increased from virtually zero when the brushes were not touching to almost 25% at a separation of 15 nm. The equivalent viscosity of a 25% PB solution would have increased by several orders of magnitude. The important distinction to note is that this experiment was predominantly sensitive to the viscous dissipation of the solvent during the pumping experiment and that the polymer molecules did not leave the gap during these measurements.

Direct measurements of solvent diffusion by NMR, as a function of polymer concentration, similarly show lowering of diffusion constants by a factor of only 2−3 over this concentration range of polymer.[30] This then agrees well with the small changes in effective viscosity observed here.

The second important point to note is that the equivalent geometry of these measurements was of a sphere and a flat plane. This implies that the separation was not uniform over the radius of the sphere. Therefore the experimentally observed hydrodynamic

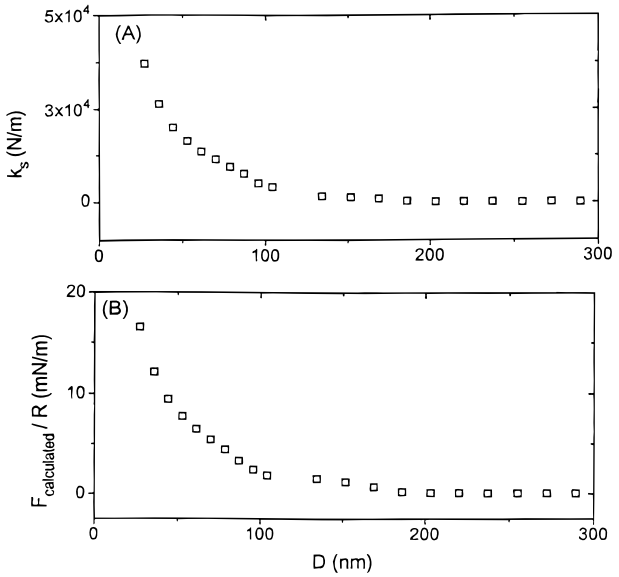

Figure 7. (A) Plot of the static force constant as a function of surface separation for PVP−PB brush-covered surfaces in tetradecane. (B) Integration of data in (A) to calculate the static force, F_{calc}, normalized by the mean radius of curvature, R, plotted against surface separation.

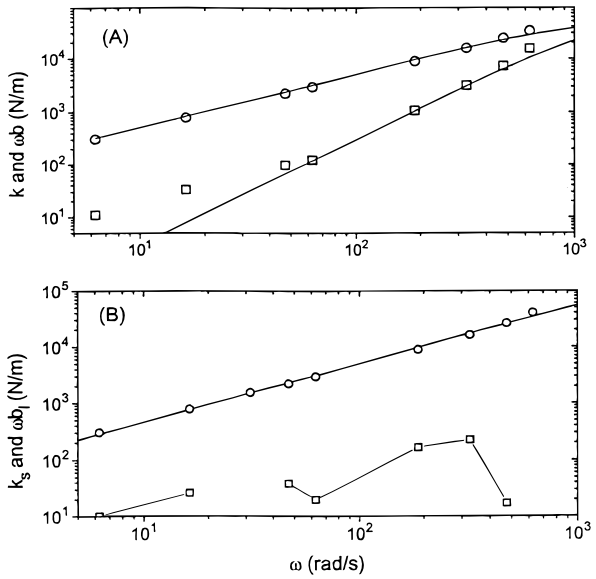

Figure 8. At surface separation 315 nm, where bulk rheological behavior holds. A plot against logarithmic frequency of the logarithmic elastic (squares) and viscous force (circles) constants inferred from small-amplitude oscillations of the film thickness. (A) Data as measured. (B) Data after analysis according to the model in Figure 3 with parameters discussed in the text. Solid lines are fits using the model shown in Figure 3.

force was integrated over various separations. As a result, the calculated changes of effective viscosity should be somewhat underpredicted as compared to the actual viscosity changes at the closest separations.

Static Forces. The responses to the oscillatory normal force could be used to determine not only the hydrodynamic forces but also the static elastic forces. In a conventional surface forces apparatus, these static forces are measured by monitoring the deflection of the spring supporting the lower surface.[31] This approach requires considerable patience and is easily affected by mechanical and thermal drifts. The elastic damping observed by the double-cantilever bimorph assembly shown in Figure 1 is not significantly affected by drifts over times of 50−100 s, however. (Incidentally, this stability could be improved using feedback loop mechanisms which have been widely developed for modern atomic force microscopes (AFMs).)

The measured elastic force constants for PVP−PB brushes in tetradecane are plotted against surface separation in Figure 7A. The k_s values started out from close to zero at large separations, as expected since the brush layers did not touch, and then increased monotonically. At the most squeezed states, the measured k_s approached the known stiffness of the apparatus. After this point, we observed a small amount of flattening of the surfaces due to the deformation of the underlying substrate.

These elastic force constants could be integrated to obtain static force, since $k_s = \mathrm{d}F/\mathrm{d}D$. The results are shown in Figure 7B. The similarity in the range and absolute magnitude of static forces obtained from this measurement to those obtained using traditional methods (see Figure 2) is striking. The difference in absolute magnitude, by a constant factor close to 4, may reflect differences in calibrating the two independent measurements. They may also, in principle, reflect frequency-dependent changes of the brush configurations, since elasticity at zero frequency need not be the same as that measured at finite frequency. Further experiments are needed to clarify this point.

Frequency Dependence. The discussion preceding this has concerned measurements at constant frequency while varying the separations between the two surfaces. In this section, we demonstrate how changes in the forcing frequency can alter the relative magnitudes of elastic and dissipative forces. This is an important issue since in a typical colloidal dispersion the Brownian motion of the particles may lead to very large approach velocities and to correspondingly large hydrodynamic forces. This could prevent flocculation even before the steric forces played a dominant role.

In Figure 8 we show the frequency response in a case that the separation was large compared to the length of the brush layers. The elastic response was negligible at low frequency but comparable to the dissipative response at high frequency. The viscous force constants, ωb, were proportional to ω as expected for a Newtonian liquid. The slope implied the known viscosity of tetradecane, 2.3 cP.

Here the anomalous elastic response can be directly traced to the compliance of the device or the glue and can be modeled using the model shown in Figure 3 with $k_s = 0$, $k_g = 1.0 \times 10^5$ N/m, and $b_L = 51$ kg/s, indicated by the solid lines in Figure 8. The k_g value obtained from the fit is in good agreement with the k_g value determined from bare mica−mica contact. As shown in the bottom panel of Figure 8, the apparent elastic contribution vanished when this was taken into account.

In Figure 9 we show the dependence on drive frequency in a case for which the separation was smaller than the brush thickness, L_0. The low-frequency elasticity came from the static forces shown in Figure 2. At high frequencies the increased elasticity came from the elastic compliance of the device and the glue. The viscoelastic response could be modeled using the model shown in Figure 3 with $k_s = 2.8 \times 10^4$ N/m, $k_G = 1 \times 10^5$ N/m, and $b_L = 680$ kg/s, indicated by the solid lines in Figure 9A.

Figure 9B shows the elastic and viscous force constants after correcting for the device compliance. The elastic response, k_s, was frequency-independent between 1 and 100 Hz as expected for elastic forces due to the

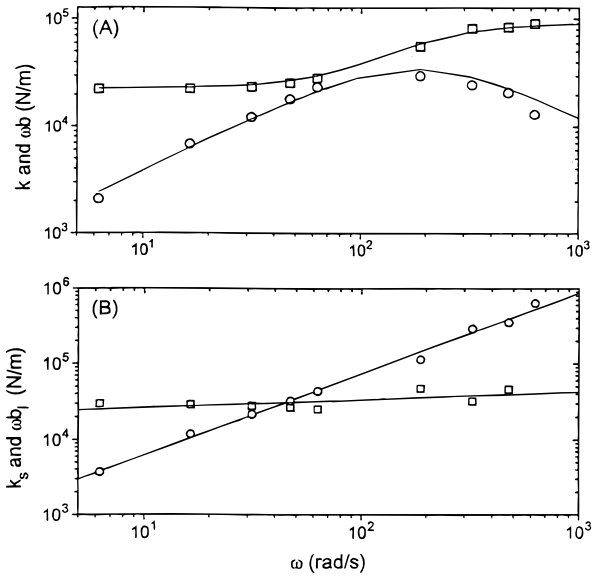

Figure 9. At surface separation 26 nm, where bulk rheological behavior holds. A plot against logarithmic frequency of the logarithmic elastic (squares) and viscous force (circles) constants inferred from small-amplitude oscillations of the film thickness. (A) Data as measured. (B) Data after analysis according to the model in Figure 3 with parameters discussed in the text. Solid lines are fits using the model shown in Figure 3.

resistance of brush layers to interpenetrate. The viscous response was proportional to frequency as expected for flow of a Newtonian liquid.

An interesting aspect is that this resulted in elastic-to-viscous response with increasing frequency: static elastic forces dominated when the frequency was low, but viscous forces grew in relative magnitude as the frequency increased. This is just the reverse of the behavior, viscous to elastic, that rheologists typically expect for (say) a Maxwell arrangement of a spring and dashpot.

On this basis, we emphasize that the point of observed crossover of dissipation and elasticity, at some frequency, need not reflect an inverse relaxation time of the sample itself, since the crossover frequency is proportional to the ratio of static and hydrodynamic forces. In experiments of the present type, the static force was due only in part to elastic compression of the brushes; it depended also upon compliance of the device itself. At the smallest separations the hydrodynamic forces were larger in relative magnitude. The contrast between Figures 8 and 9 illustrates that this lowered the observed crossover frequency.

Conclusions

In summary, we have measured the elastohydrodynamic forces due to drainage of a good solvent between solid surfaces coated with a polymer brush. Analysis was simplified by the fact that because the brush appeared to give a negligibly small dissipative response over the frequencies studied (as manifested by frequency-independent elasticity), the observed dissipation could be attributed to solvent flow.

So long as the separation, D, was substantially greater than the unperturbed length of the brush, L_0, the magnitudes of hydrodynamic forces could be modeled using the Reynolds equation. However, at $D < 4L_0$, rather far before the opposing brushes touched one another, the effective hydrodynamic thickness was observed to decrease with diminishing surface separation. For $D < 2L_0$, the hydrodynamic forces scaled empirically as $D^{-1.2}$.

The frequency response indicated a progressive crossover from elastic to viscous response with increasing frequency; but this could be fully explained as the combination of mechanical influences from the device itself, static structural forces (i.e. the force−distance profile), and hydrodynamic forces due to drainage of the liquid from the gap. True confinement-induced solid-like behavior was observed for separations very close to the dry-layer thickness, $D \approx 6$ nm.

This ultimate solidity was probed more conveniently by shear rheology, as discussed elsewhere.[33,34]

There remain several challenges for future work. Quantitative understanding of how far the solvent velocity field penetrated within the brush layers, especially under circumstances where $D > 2L_0$ so that a layer of pure solvent should have separated the opposed brushes, is not yet in hand. On the experimental side, the effects of shear on static and hydrodynamic forces are currently in progress. Above all, in future work, it will be interesting to understand quantitatively why the hydrodynamic radius decreased so monotonically with surface separation, with no clear change of trend at the point where the brushes began to overlap. The observed scaling of hydrodynamic forces with $D^{-1.2}$ could reflect different scaling behavior of the static and hydrodynamic screening lengths or could reflect inapplicability of the Brinkman equation to understand solvent permeability in polymer layers.

Acknowledgment. We are indebted to Professor H. Watanabe for donating the PB−PVP sample and to Lenore L. Cai for measuring the static force−distance profile. This work was supported by grants from the Exxon Research and Engineering Co. and the U.S. Air Force (AFOSR-URI-F49620-93-1-02-41).

References and Notes

(1) Napper, D. H. *Polymeric Stabilization of Colloidal Dispersions*; Academic Press: London, 1983.
(2) Russell, W. B.; Saville, D. A.; Schowalter, W. R. *Colloidal Dispersions*; Cambridge University Press: New York, 1989.
(3) Alexander, S. *J. Phys. (Paris)* **1977**, *38*, 977.
(4) de Gennes, P.-G. *J. Phys. (Paris)* **1976**, *37*, 1443.
(5) Milner, S. T.; Witten, T. A.; Cates, M. E. *Macromolecules* **1988**, *21*, 2610.
(6) Skvortsov, A. M.; Gorbunov, A. A.; Parlushkov, I. V.; Zhulina, E. B.; Borisov, O. V.; Priamitsyn, V. A. *Vysokomol. Soedin. Ser. A* **1988**, *30*, 1615.
(7) Milner, S. T. *Science* **1991**, *251*, 905.
(8) Rabin, Y.; Alexander, S. *Europhys. Lett.* **1990**, *13*, 49.
(9) Taunton, H. J.; Toprakcioglu, C.; Fetters, L. J.; Klein, J. *Nature* **1988**, *332*, 712.
(10) Taunton, H. J.; Toprakcioglu, C.; Fetters, L. J.; Klein, J. *Macromolecules* **1990**, *23*, 571.
(11) Patel, S.; Tirrell, M. *Annu. Rev. Phys. Chem.* **1989**, *40*, 597.
(12) Klein, J. *J. Chem. Soc., Faraday Trans. 1* **1983**, *79*, 99.
(13) Auroy, P.; Auray, L.; Leger, L. *J. Colloid Interface Sci.* **1992**, *150*, 187.
(14) Auroy, P.; Mir, Y.; Auvray, L. *Phys. Rev. Lett.* **1992**, *69*, 93.
(15) Reynolds, O. *Philos. Trans. R. Soc. London* **1986**, *177*, 157.
(16) Israelachvili, J. N. *Pure Appl. Chem.* **1988**, *60*, 1473.
(17) Klein, J.; Kaiyama, Y.; Yoshizawa, H.; Israelachvili, J. N.; Fredrickson, G. H.; Pincus, P.; Fetters, L. J. *Macromolecules* **1993**, *26*, 5552.
(18) Georges, J. M.; Millot, S.; Loubet, J. L.; Tonck, A. *J. Chem. Phys.* **1993**, *98*, 7345.
(19) Moore, D. F. *Principles and Applications of Tribology*; Pergamon Press: New York, 1975.
(20) Milner, S. T. *Macromolecules* **1991**, *24*, 3704.
(21) Fredrickson, G. H.; Pincus, P. *Langmuir* **1991**, *7*, 786.

(22) Harden, J. L.; Pleiner, H.; Pincus, P. A. *Langmuir* **1989**, *5*, 1436.
(23) Peachey, J.; Van Alsten, J.; Granick, S. *Rev. Sci. Instrum.* **1991**, *62*, 463.
(24) Montfort, J. P.; Hadziioannou, G. *J. Chem. Phys.* **1988**, *88*, 7187.
(25) Israelachvili, J. N.; Kott, S. J. *J. Colloid Interface Sci.* **1989**, *129*, 461.
(26) Dhinojwala, A.; Granick, S. *J. Chem. Soc., Faraday Trans.* **1996**, *92*, 619.
(27) Brinkman, H. C. *Appl. Sci. Res.* **1947**, *A1*, 27.
(28) Fredrickson, G. H., personal communication.
(29) Ferry, J. D. *Viscoelastic Properties of Polymers*, 3rd ed.; Wiley: New York, 1980.
(30) Pelletier, E.; Montfort, J. P.; Loubet, J. L.; Tonck, A.; Georges, J. M. *Macromolecules* **1995**, *28*, 1990.
(31) Von Meerwall, E. D. *Adv. Polym. Sci.* **1983**, *54*, 1.
(32) Israelachvili, J. N. *Intermolecular and Surface Forces*, 2nd ed.; Wiley: New York, 1990.
(33) Cai, L.; Dhinojwala, A.; Granick, S., submitted.
(34) Dhinojwala, A.; Cai, L.; Granick, S. *Langmuir* **1996**, *12*, 4537.

MA960027W